Structural Engineering and Mechanics, *Vol. 74, No. 6 (2020) 809-819*
DOI: https://doi.org/10.12989/sem.2020.74.6.809

Elastic wave characteristics of graphene nanoplatelets reinforced composite nanoplates

Behrouz Karami*[1], Parastoo Gheisari[2], Seyed Mohammad Reza Nazemosadat[3], Payam Akbari[4], Davood Shahsavari[1] and Matin Naghizadeh[5]

[1]*Department of Mechanical Engineering, Marvdasht Branch, Islamic Azad University, Marvdasht, Iran*
[2]*School of Mechanical Engineering, Shiraz University, Shiraz, Iran*
[3]*Sama Technical and Vocational Training College, Islamic Azad University, Shiraz Branch, Shiraz, Iran*
[4]*Department of Civil Engineering, Tehran South Branch, Islamic Azad University, Tehran, Iran*
[5]*Department of Chemistry, Shahid Bahonar University of Kerman, Kerman, Iran*

(Received August 13, 2019, Revised January 31, 2020, Accepted February 4, 2020)

Abstract. For the first time, the influence of in-plane magnetic field on wave propagation of Graphene Nano-Platelets (GNPs) polymer composite nanoplates is investigated here. The impact of three- parameter Kerr foundation is also considered. There are two different reinforcement distribution patterns (i.e. uniformly and non-uniformly) while the material properties of the nanoplate are estimated through the Halpin-Tsai model and a rule of mixture. To consider the size-dependent behavior of the structure, Eringen Nonlocal Differential Model (ENDM) is utilized. The equations of wave motion derived based on a higher-order shear deformation refined theory through Hamilton's principle and an analytical technique depending on Taylor series utilized to find the wave frequency as well as phase velocity of the GNPs reinforced nanoplates. A parametric investigation is performed to determine the influence of essential phenomena, such as the nonlocality, GNPs conditions, Kerr foundation parameters, and wave number on the both longitudinal and flexural wave characteristics of GNPs reinforced nanoplates.

Keywords: wave propagation; nanocomposite plate; graphene nanoplatlets; magnetic field; Kerr foundation

1. Introduction

Wave propagation appears for multi-conceptualization physical phenomena, containing geophysics, blood flow, acoustics, hydrodynamics, non-destructive evaluation, and further applications in which waves are travelling in the demanding directions. For researchers who work on the ultrasonic inspection techniques and structural health monitoring, an adequate information on wave propagation response is one of the crucial necessities for varying material properties and geometries.

As far as material properties is concerned, reinforced materials or structures have been widely considered by designers around the world (Jawaid, Thariq *et al*. 2018), because of the remarkable properties of the structure (i.e. high strength and stiffness). Hence, many structural analysis have performed effort to study on mechanical behavior of these structures so far (Mehar and Panda 2016, Bakhadda, Bouiadjra *et al*. 2018, Draoui, Zidour *et al*. 2019, Kar, Panda *et al*. 2019, Medani, Benahmed *et al*. 2019, Mehar and Panda 2019, Mehar and Panda 2019, Mehar, Panda *et al*. 2019). Generally speaking, a polymeric composite matrix can be reinforced with carbon nanotube, Graphene or Graphene Platelets (GPLs). However, as reported by (Rafiee, Rafiee *et al*. 2009), the strength and stiffness obtained by carbon nanotubes with 1% weight fraction can be achieved for GPLs by adding only 0.1% weight fraction.

Graphene as the thinnest two-dimensional material, which its thickness is only 0.34 nm, contains internal actions of atoms, known as the ‘‘size effect’’ which must be identified and estimated for exact analysis. In fact, experimental, molecular dynamics (MD) simulation and non-classical continuum theories are the main methods for estimating the role of size-dependent effects in which the third can be considered as the most efficient due to devoted time and effort. Classical continuum theories such as Kirchhoff plate theory, Three-Dimensional (3D) elasticity theory, various types of higher-order shear deformation theories (Dutta, Panda *et al*. 2017, Bourada, Amara *et al*. 2018, Dash, Mehar *et al*. 2018, Fourn, Atmane *et al*. 2018, Boulefrakh, Hebali *et al*. 2019, Bourada, Bousahla *et al*. 2019, Chaabane, Bourada *et al*. 2019, Dash, Mehar *et al*. 2019, Meksi, Benyoucef *et al*. 2019, Ramteke, Panda *et al*. 2019), and multiple quasi-3D shear deformation theories (Boukhlif, Bouremana *et al*. 2019, Mahmoudi, Benyoucef *et al*. 2019, Zaoui, Ouinas *et al*. 2019, Zarga, Tounsi *et al*. 2019), are unable to predict the behavior of structures when the dimensions of the structure tend to the nanoscale. Therefore, there is a necessity to rewrite the classical relations by adding the small-scale parameters. To overcome this problem, some non-classical continuum theories have been developed and reported such as Eringen nonlocal model (Zemri, Houari *et al*. 2015, Bounouara, Benrahou *et al*. 2016, Bellifa, Benrahou *et al*. 2017, Kaghazian, Hajnayeb *et al*. 2017, Khetir, Bouiadjra *et al*. 2017, Bensaid and Bekhadda 2018, Bensaid, Bekhadda *et*

*Corresponding author, Senior Lecturer
E-mail: behrouz.karami@miau.ac.ir

ISSN: 1225-4568 (Print), 1598-6217 (Online)

al. 2018, Bouadi, Bousahla *et al*. 2018, Hosseini, Bahaadini *et al*. 2018, Mehar, Mahapatra *et al*. 2018, Mokhtar, Heireche *et al*. 2018, Rahmani, Deyhim *et al*. 2018, Yazid, Heireche *et al*. 2018, Youcef, Kaci *et al*. 2018, Berghouti, Adda Bedia *et al*. 2019, Boutaleb, Benrahou *et al*. 2019, Gao, Xiao *et al*. 2019), strain gradient model with one parameter (Papargyri-Beskou, Polyzos *et al*. 2009, Ghayesh, Amabili *et al*. 2013, Akgöz and Civalek 2014, Alimirzaei, Mohammadimehr *et al*. 2019), modified couple stress models (Ghayesh, Amabili *et al*. 2013, Kocaturk and Akbas 2013, Farokhi and Ghayesh 2015, Ghayesh, Farokhi *et al*. 2016, Ghayesh, Farokhi *et al*. 2017, Ghayesh and Farokhi 2018, Ghayesh, Farokhi *et al*. 2018, Wang and Zheng 2018), and nonlocal strain gradient model (Barati and Shahverdi 2017, Karami, Janghorban *et al*. 2017, Karami, Janghorban *et al*. 2018, Karami, Janghorban *et al*. 2018, Karami, Janghorban *et al*. 2018, Karami, Shahsavari *et al*. 2018, Karami, Janghorban *et al*. 2019, Karami, Shahsavari *et al*. 2019).

Among the above theories, "the differential equation consequent (but not equivalent) to Eringen strain-driven nonlocal elasticity theory (Eringen and Edelen 1972, Eringen 1983) has been generally used as a constitutive law for modeling nanoscale devices and systems (Romano, Barretta *et al*. 2017)". The strain-driven nonlocal integral theory assumes that the strain at a point depends on both stress and spatial derivatives of the stress at that point. Of course, it's worth noting that the strain-driven integral law is not continuously adapted to investigate the nano scale structures defined on bounded domains. (Romano and Barretta 2017) presented an effective model to study the basic mechanics of nanobeams. In order to simplify the relations, researchers have conducted multiple mechanical studies via Eringen strain-driven nonlocal differential model. Forced vibrations of the nanoplate including the moving load were presented by (Shahsavari and Janghorban 2017) based on refined plate theory. In another work (Shahsavari, Karami *et al*. 2017) investigated the hygrothermal effects on the dynamic response of viscoelastic nanoplates considering moving load via Eringen's nonlocal model. Vibrational response of bi-directional Functionally Graded (FG) nanosize tubes were reported by (Li and Hu 2017) via Eringen nonlocal model. Guided wave propagation behavior of porous materials for rectangular nanoplates were reported by (Karami, Janghorban *et al*. 2018) via Eringen nonlocal model. Thermo-mechanical vibration of FG nanobeam were investigated by (Ebrahimi, Barati *et al*. 2018) based upon a new Eringen nonlocal model. Buckling response of nanotubes made of silicon carbide including surface effect via Eringen nonlocal model were investigated by (Mercan and Civalek 2017).

Static, dynamic, and stability analysis of GNPs reinforced polymer composite plates are plenty; however, there is no study on the wave propagation of GNPs reinforced polymer composite plates. A structural vibration analysis of GNPs reinforced composite plates was presented by (Song, Kitipornchai *et al*. 2017) via the First-Order Shear Deformation Plate Theory (FSDT) that solved by Navier solution based technique. Moreover, (Song, Yang *et al*. 2018) studied the statics as well as stability of GNPs reinforced composite plates using the FSDT. An study on nonlinear vibration of GNPs reinforced composite plates was conducted by (Gholami and Ansari 2018) based on a unified higher-order model. Recently, (Arefi, Bidgoli *et al*. 2018) investigated the size-dependent free vibrations of GNPs reinforced composite nanoplates based on a two-variable sinusoidal shear deformation theory and Eringen's nonlocal model. Small-scale effects on the nonlinear large-amplitude vibrations of GNPs reinforced porous micro/nano-plates were studied by (Sahmani, Aghdam *et al*. 2018) for the first time. And in another work (Sahmani, Aghdam *et al*. 2018) analyzed the nonlinear axial instability of the structure.

Owing to the lack of an investigations on the wave propagation analysis of GNPs reinforced composite nanoplates, the objective of the current work is to model the wave propagation behavior of the structure under in-plane magnetic field considering three-parameter elastic foundation (as known Kerr foundation). Different GNPs reinforcement distributions scheme are also studied. Halpin-Tsai model and a rule of mixture are utilized to estimate the material properties of the structure. In order to examine the size-dependent wave behavior of nanostructure systems, Eringen nonlocal differential model is adopted. Equations of wave motion are obtained via a refined plate theory and solved analytically for wave propagation phenomenon. Then, the impact of significant parameters on the wave characteristics of the nanoplates, such as the nonlocality, GNPs components, wave number and elastic foundation are analyzed using parametric examples.

2. Eringen nonlocal differential model

The stress tensor for strain-driven nonlocal elasticity is given by (Eringen 1983),

$$\tau_{ij} = \int_V \alpha(|x'-x|,\tau)\sigma_{ij}(x')d(V') \tag{1}$$

where σ_{ij} and τ_{ij} are respectively the local and nonlocal stress tensors.

In current study, the following differential model is utilized to consider the small-scale effects,

$$\left(1-(e_0a)^2\nabla^2\right)\sigma_{ij} = C_{ijkl}\varepsilon_{kl} \tag{2}$$

herein ∇^2 is the Laplacian operator.

3. Basic formulation

3.1 Functionally graded polymer composite nanoplate reinforced with GNPs

Suppose configuration of a nanoplate made of polymeric composite materials with the length of a, width b, and thickness h which is made of N_L layers with the thickness $\delta h=h/N_L$ as Fig. 1. To consider the filler inside each layer, the Graphene Nano-Platelets (GNPs) are used due to the

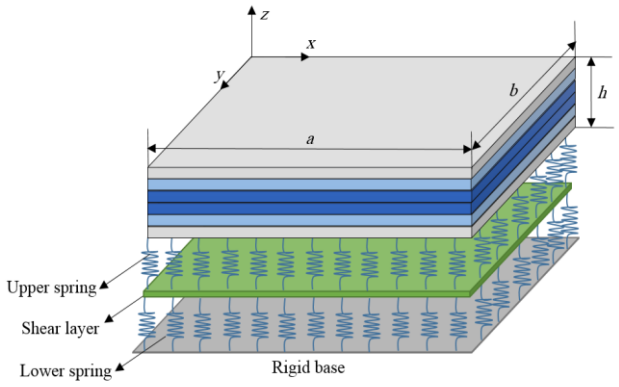

Fig. 1 The geometry of GNPs reinforced polymer composite nanoplate resting on Kerr foundation

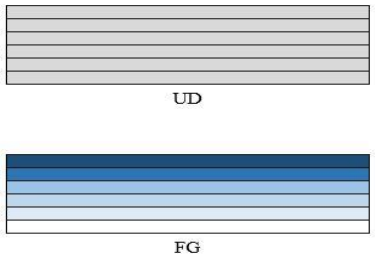

Fig. 2 Patterns of FG materials

two different distribution schemes as uniformaly and non-uniformly distribution (UD and FG) see in Fig. 2.

The nanoplate's Young modulus is as follows (Affdl and Kardos 1976)

$$E_c^{(k)} = \frac{3}{8}\frac{1+\xi_L\eta_L V_{GNP}^{(k)}}{1-\eta_L V_{GNP}^{(k)}} \times E_M + \frac{5}{8}\frac{1+\xi_W\eta_W V_{GNP}^{(k)}}{1-\eta_W V_{GNP}^{(k)}} \times E_M \tag{3}$$

herein the GNP and polymer matrix Young moduli are respectively represent by E_M and E_{GNP}; $V_{GNP}^{(k)}$ is GNP's volume fraction and defined as follows

$$V_{GNP}^{(k)} = \frac{g_{GNP}^{(k)}}{g_{GNP}^{(k)} + (\rho_{GNP}/\rho_M)(1-g_{GNP}^{(k)})} \tag{4}$$

in which $g_{GNP}^{(k)}$ is the weight fraction; ρ_{GNP} and ρ_M denote the density of GNPs and polymer, respectively. Density and Poisson ratio for the k-layer GNPs reinforced composite nanoplates are defined as follow

$$\rho_c^{(k)} = \rho_{GNP} V_{GNP}^{(k)} + \rho_M V_M^{(k)} \tag{5}$$

$$\nu_c^{(k)} = \nu_{GNP} V_{GNP}^{(k)} + \nu_M V_M^{(k)} \tag{6}$$

where ν_M and ν_{GNP} refer to the Poisson ratio of polymer matrix and GNPs, respectively and two additional parameters (η_L, η_W) are defined as

$$\eta_L = \frac{(E_{GNP}/E_M)-1}{(E_{GNP}/E_M)+\xi_L} \tag{7}$$

$$\eta_L = \frac{(E_{GNP}/E_M)-1}{(E_{GNP}/E_M)+\xi_W} \tag{8}$$

in which ξ_L and ξ_W depend on the geometry as well as size of the GNP nanofillers as below

$$\xi_L = 2(l_{GNP}/h_{GNP}) \tag{9}$$

$$\xi_W = 2(w_{GNP}/h_{GNP}) \tag{10}$$

where l_{GNP}, w_{GNP}, and h_{GNP} are the average length, width, and thickness of the GNPs, respectively. The weight fraction of GNPs for two different distribution schemes are computed as follows (Song, Yang *et al*. 2018)

$$g_{GNP}^{(k)} = \begin{cases} g_{GNP}^* & \text{UD} \\ 2kg_{GNP}^*/(N_L+1) & \text{FG} \end{cases} \tag{11}$$

3.2 Kinematic relations

To investigate the wave propagation of the nanoplate, following displacement field are considered (Ebrahimi, Barati *et al*. 2016):

$$\begin{aligned} u(x,y,z,t) &= u_0(x,y,t) - z\frac{\partial w_b}{\partial x} - f(z)\frac{\partial w_s}{\partial x} \\ v(x,y,z,t) &= v_0(x,y,t) - z\frac{\partial w_b}{\partial y} - f(z)\frac{\partial w_s}{\partial y} \\ w(x,y,z,t) &= w_b(x,y,t) + w_s(x,y,t) \end{aligned} \tag{12}$$

where f(z) is the shape function and presented as follows

$$f(z) = -z/4 + \frac{5}{3}z(z/h)^2 \tag{13}$$

The linear constitutive stress-strain relations for a k-layer polymer composite nanoplate can be written as:

$$(1-\mu^2\nabla^2)\begin{bmatrix}\sigma_x\\ \sigma_y\\ \tau_{yz}\\ \tau_{xz}\\ \tau_{xy}\end{bmatrix} = \begin{bmatrix} C_{11}^{(k)} & C_{12}^{(k)} & 0 & 0 & 0 \\ C_{12}^{(k)} & C_{22}^{(k)} & 0 & 0 & 0 \\ 0 & 0 & C_{44}^{(k)} & 0 & 0 \\ 0 & 0 & 0 & C_{55}^{(k)} & 0 \\ 0 & 0 & 0 & 0 & C_{66}^{(k)} \end{bmatrix}\begin{bmatrix}\varepsilon_x\\ \varepsilon_y\\ \gamma_{yz}\\ \gamma_{xz}\\ \gamma_{xy}\end{bmatrix} \tag{14}$$

where

$$\begin{aligned} C_{11}^{(k)} &= C_{22}^{(k)} = \frac{E_c^{(k)}}{1-(\nu_c^{(k)})^2} \\ C_{12}^{(k)} &= C_{21}^{(k)} = \nu_c^{(k)} C_{11}^{(k)} \\ C_{44}^{(k)} &= C_{55}^{(k)} = C_{66}^{(k)} = G(z) = \frac{E_c^{(k)}}{2(1+\nu_c^{(k)})} \end{aligned} \tag{15}$$

and μ=e_0a.

Non-zero strain-displacement relations are defined as follows:

$$\begin{Bmatrix}\varepsilon_x\\ \varepsilon_y\\ \gamma_{xy}\end{Bmatrix}=\begin{Bmatrix}\varepsilon_x^0\\ \varepsilon_y^0\\ \gamma_{xy}^0\end{Bmatrix}+z\begin{Bmatrix}k_x^b\\ k_y^b\\ k_{xy}^b\end{Bmatrix}+f(z)\begin{Bmatrix}k_x^s\\ k_y^s\\ k_{xy}^s\end{Bmatrix}$$
$$\begin{Bmatrix}\gamma_{yz}\\ \gamma_{xz}\end{Bmatrix}=g\begin{Bmatrix}\gamma_{yz}^0\\ \gamma_{xz}^0\end{Bmatrix},\ g=1-\frac{\partial f}{\partial z} \tag{16}$$

where

$$\begin{Bmatrix}\varepsilon_x^0\\ \varepsilon_y^0\\ \gamma_{xy}^0\end{Bmatrix}\begin{Bmatrix}\frac{\partial u_0}{\partial x}\\ \frac{\partial v_0}{\partial y}\\ \frac{\partial u_0}{\partial y}+\frac{\partial v_0}{\partial x}\end{Bmatrix},\ \begin{Bmatrix}k_x^b\\ k_y^b\\ k_{xy}^b\end{Bmatrix}=\begin{Bmatrix}-\frac{\partial^2 w_b}{\partial x^2}\\ -\frac{\partial^2 w_b}{\partial y^2}\\ -2\frac{\partial^2 w_b}{\partial x\,\partial y}\end{Bmatrix}$$
$$\begin{Bmatrix}k_x^s\\ k_y^s\\ k_{xy}^s\end{Bmatrix}=\begin{Bmatrix}-\frac{\partial^2 w_s}{\partial x^2}\\ -\frac{\partial^2 w_s}{\partial y^2}\\ -2\frac{\partial^2 w_s}{\partial x\,\partial y}\end{Bmatrix},\begin{Bmatrix}\gamma_{yz}^0\\ \gamma_{xz}^0\end{Bmatrix}=\begin{Bmatrix}\frac{\partial w_s}{\partial y}\\ \frac{\partial w_s}{\partial x}\end{Bmatrix} \tag{17}$$

Owing to Hamilton's principle, the equations of motion can be defined as follows:

$$\int_0^t \delta(U-K+V)dt=0 \tag{18}$$

where U and K refer, respectively, to the strain and kinetic energies and δV denotes the applied forces. The variation of strain energy is defined as

$$\begin{aligned}\delta U&=\int_{-h/2}^{h/2}\int_A\left[\sigma_x\delta\varepsilon_x+\sigma_y\delta\varepsilon_y+\tau_{yz}\varepsilon_{yz}+\tau_{xz}\varepsilon_{xz}+\tau_{xy}\varepsilon_{xy}\right]dAdz\\&=\int_A\left[N_x\delta\varepsilon_x^0+N_y\delta\varepsilon_y^0+N_{xy}\delta\gamma_{xy}^0+M_x^b\delta k_x^b+M_y^b\delta k_y^b+M_{xy}^b\delta k_{xy}^b\right.\\&\left.+M_x^s\delta k_x^s+M_y^s\delta k_y^s+M_{xy}^s\delta k_{xy}^s+Q_{yz}^s\gamma_{yz}^0+Q_{xz}^s\gamma_{xz}^0\right]dA=0\end{aligned} \tag{19}$$

herein the variables at the last expression are defined by:

$$\begin{Bmatrix}N_x & N_y & N_z\\ M_x^b & M_y^b & M_{xy}^b\\ M_x^s & M_y^s & M_{xy}^s\end{Bmatrix}=\int_{-h/2}^{h/2}(\sigma_x,\sigma_y,\tau_{xy})\begin{Bmatrix}1\\ z\\ f\end{Bmatrix}dz \tag{20}$$

and

$$(Q_{xz}^s,Q_{yz}^s)\int_{-h/2}^{h/2}g(\tau_{xz},\tau_{yz})dz \tag{21}$$

The kinetic energy variations can be written as following form:

$$\begin{aligned}\delta K=\int_A\Big\{&I_0\Big(\frac{\partial u_0}{\partial t}\frac{\partial\delta u_0}{\partial t}+\frac{\partial v_0}{\partial t}\frac{\partial\delta v_0}{\partial t}+\Big(\frac{\partial w_b}{\partial t}+\frac{\partial w_s}{\partial t}\Big)\Big(\frac{\partial\delta w_b}{\partial t}+\frac{\partial\delta w_s}{\partial t}\Big)\Big)\\&-I_1\Big(\frac{\partial u_0}{\partial t}\frac{\partial^2\delta w_b}{\partial t\partial x}+\frac{\partial^2 w_b}{\partial t\partial x}\frac{\partial\delta u_0}{\partial t}+\frac{\partial v_0}{\partial t}\frac{\partial^2\delta w_b}{\partial t\partial y}+\frac{\partial^2 w_b}{\partial t\partial y}\frac{\partial\delta v_0}{\partial t}\Big)\\&-J_1\Big(\frac{\partial u_0}{\partial t}\frac{\partial^2\delta w_s}{\partial t\partial x}+\frac{\partial^2 w_s}{\partial t\partial x}\frac{\partial\delta u_0}{\partial t}+\frac{\partial v_0}{\partial t}\frac{\partial^2\delta w_s}{\partial t\partial y}+\frac{\partial^2 w_s}{\partial t\partial y}\frac{\partial\delta v_0}{\partial t}\Big)\\&+I_2\Big(\frac{\partial^2 w_b}{\partial t\partial x}\frac{\partial^2\delta w_b}{\partial t\partial x}+\frac{\partial^2 w_b}{\partial t\partial y}\frac{\partial^2\delta w_b}{\partial t\partial y}\Big)+K_2\Big(\frac{\partial^2 w_s}{\partial t\partial x}\frac{\partial^2\delta w_s}{\partial t\partial x}+\frac{\partial^2 w_s}{\partial t\partial y}\frac{\partial^2\delta w_s}{\partial t\partial y}\Big)\\&+J_2\Big(\frac{\partial^2 w_b}{\partial t\partial x}\frac{\partial^2\delta w_b}{\partial t\partial x}+\frac{\partial^2 w_s}{\partial t\partial x}\frac{\partial^2\delta w_s}{\partial t\partial x}+\frac{\partial^2 w_b}{\partial t\partial y}\frac{\partial^2\delta w_b}{\partial t\partial y}+\frac{\partial^2 w_s}{\partial t\partial y}\frac{\partial^2\delta w_s}{\partial t\partial y}\Big)\Big\}dA\end{aligned} \tag{22}$$

where (I_0, I_1, J_1, I_2, J_2, K_2) are mass inertias introduced as below:

$$\{I_0,I_1,J_1,I_2,J_2,K_2\}=\sum_{k=1}^{N_L}\int_{z(k)}^{z(k+z)}\{1,z,f,z^2,zf,f^2\}\rho_c^{(k)}dz \tag{23}$$

3.3 Kerr elastic foundation model

The relation of a three-parameter elastic foundation including a shear layer and two linear layer which is known as Kerr model, is expressed as (Rad 2015),

$$q_{\text{Kerr}}-\Big(\frac{k_s}{k_l+k_u}\Big)\nabla^2 q_{\text{Kerr}}=\Big(\frac{k_l k_u}{k_l+k_u}\Big)w-\Big(\frac{k_s k_u}{k_l+k_u}\Big)\nabla^2 w \tag{24}$$

The first variation of work done can be obtained as:

$$\delta V=\int_{-h/2}^{h/2}\int_A\left[\eta h H_x^2\nabla^2\delta w+q_{\text{Kerr}}\delta w\right]dAdz \tag{25}$$

where η represents the magnetic permeability, and H_x is the magnetic potential. By inserting Eqs. (19), (22), and (25) into Eq. (18), and setting the coefficients of δu_0, δv_0, δw_b, and δw_s to zero, the following equations can be found

$$\delta u_0:\frac{\partial N_x}{\partial x}+\frac{\partial N_{xy}}{\partial y}=I_0\frac{\partial^2 u_0}{\partial t^2}-I_1\frac{\partial^3 w_b}{\partial x\,\partial t^2}-J_1\frac{\partial^3 w_s}{\partial x\,\partial t^2} \tag{26}$$

$$\delta v_0:\frac{\partial N_{xy}}{\partial x}+\frac{\partial N_y}{\partial y}=I_0\frac{\partial^2 v_0}{\partial t^2}-I_1\frac{\partial^3 w_b}{\partial y\,\partial t^2}-J_1\frac{\partial^3 w_s}{\partial y\,\partial t^2} \tag{27}$$

$$\begin{aligned}&\delta w_b:\frac{\partial^2 M_x^b}{\partial x^2}+2\frac{\partial^2 M_{xy}^b}{\partial x\,\partial y}+\frac{\partial^2 M_y^b}{\partial y^2}-\Big(\frac{k_l k_u}{k_l+k_u}\Big)(w_b+w_s)\\&+\Big(\frac{k_s k_u}{k_l+k_u}+\eta h H_x^2\Big)\Big(\frac{\partial^2(w_b+w_s)}{\partial x^2}+\frac{\partial^2(w_b+w_s)}{\partial y^2}\Big)\\&=I_0\Big(\frac{\partial^2 w_b}{\partial t^2}+\frac{\partial^2 w_s}{\partial t^2}\Big)+I_1\Big(\frac{\partial^3 u_0}{\partial x\,\partial t^2}+\frac{\partial^3 v_0}{\partial y\,\partial t^2}\Big)-I_2\Big(\frac{\partial^4 w_b}{\partial x^2\partial t^2}+\frac{\partial^4 w_b}{\partial y^2\partial t^2}\Big)\\&-J_2\Big(\frac{\partial^4 w_s}{\partial x^2\partial t^2}+\frac{\partial^4 w_s}{\partial y^2\partial t^2}\Big)\end{aligned} \tag{28}$$

$$\begin{aligned}&\delta w_s:\frac{\partial^2 M_x^s}{\partial x^2}+2\frac{\partial^2 M_{xy}^s}{\partial x\,\partial y}+\frac{\partial^2 M_y^s}{\partial y^2}+\frac{\partial Q_{xz}^s}{\partial x}+\frac{\partial Q_{yz}^s}{\partial y}\\&-\Big(\frac{k_l k_u}{k_l+k_u}\Big)(w_b+w_s)+\Big(\frac{k_s k_u}{k_l+k_u}+\eta h H_x^2\Big)\Big(\frac{\partial^2(w_b+w_s)}{\partial x^2}+\frac{\partial^2(w_b+w_s)}{\partial y^2}\Big)\\&=I_0\Big(\frac{\partial^2 w_b}{\partial t^2}+\frac{\partial^2 w_s}{\partial t^2}\Big)+J_1\Big(\frac{\partial^3 u_0}{\partial x\,\partial t^2}+\frac{\partial^3 v_0}{\partial y\,\partial t^2}\Big)-J_2\Big(\frac{\partial^4 w_b}{\partial x^2\partial t^2}+\frac{\partial^4 w_b}{\partial y^2\partial t^2}\Big)\\&-J_2\Big(\frac{\partial^4 w_s}{\partial x^2\partial t^2}+\frac{\partial^4 w_s}{\partial y^2\partial t^2}\Big)\end{aligned} \tag{29}$$

According to the stress-strain relations (Eq. (14)) and governing equations (Eqs. (26-29)), the stress resultants are obtained as:

$$\begin{Bmatrix} N \\ M^b \\ M^s \end{Bmatrix} = \begin{bmatrix} A_{11} & A_{12} & 0 \\ A_{11} & A_{12} & 0 \\ 0 & 0 & A_{66} \end{bmatrix} \begin{Bmatrix} \dfrac{\partial u}{\partial x} \\ \dfrac{\partial v}{\partial y} \\ \dfrac{\partial u}{\partial y} + \dfrac{\partial v}{\partial x} \end{Bmatrix} + \begin{bmatrix} B_{11} & B_{12} & 0 \\ B_{11} & B_{12} & 0 \\ 0 & 0 & B_{66} \end{bmatrix} \begin{Bmatrix} -\dfrac{\partial^2 w_b}{\partial x^2} \\ \dfrac{\partial^2 w_b}{\partial y^2} \\ -2\dfrac{\partial^2 w_b}{\partial x \partial y} \end{Bmatrix}$$
$$+ \begin{bmatrix} B_{11}^s & B_{12}^s & 0 \\ B_{11}^s & B_{12}^s & 0 \\ 0 & 0 & B_{66}^s \end{bmatrix} \begin{Bmatrix} -\dfrac{\partial^2 w_s}{\partial x^2} \\ \dfrac{\partial^2 w_s}{\partial y^2} \\ -2\dfrac{\partial^2 w_s}{\partial x \partial y} \end{Bmatrix} \tag{30}$$

$$\begin{Bmatrix} M_x^b \\ M_y^b \\ M_{xy}^b \end{Bmatrix} = \begin{bmatrix} B_{11} & B_{12} & 0 \\ B_{11} & B_{12} & 0 \\ 0 & 0 & B_{66} \end{bmatrix} \begin{Bmatrix} \dfrac{\partial u}{\partial x} \\ \dfrac{\partial v}{\partial y} \\ \dfrac{\partial u}{\partial y} + \dfrac{\partial v}{\partial x} \end{Bmatrix} + \begin{bmatrix} D_{11} & D_{12} & 0 \\ D_{11} & D_{12} & 0 \\ 0 & 0 & D_{66} \end{bmatrix} \begin{Bmatrix} -\dfrac{\partial^2 w_b}{\partial x^2} \\ \dfrac{\partial^2 w_b}{\partial y^2} \\ -2\dfrac{\partial^2 w_b}{\partial x \partial y} \end{Bmatrix}$$
$$+ \begin{bmatrix} D_{11}^s & D_{12}^s & 0 \\ D_{11}^s & D_{12}^s & 0 \\ 0 & 0 & D_{66}^s \end{bmatrix} \begin{Bmatrix} -\dfrac{\partial^2 w_s}{\partial x^2} \\ \dfrac{\partial^2 w_s}{\partial y^2} \\ -2\dfrac{\partial^2 w_s}{\partial x \partial y} \end{Bmatrix} \tag{31}$$

$$\begin{Bmatrix} M_x^s \\ M_y^s \\ M_{xy}^s \end{Bmatrix} = \begin{bmatrix} B_{11}^s & B_{12}^s & 0 \\ B_{11}^s & B_{12}^s & 0 \\ 0 & 0 & B_{66}^s \end{bmatrix} \begin{Bmatrix} \dfrac{\partial u}{\partial x} \\ \dfrac{\partial v}{\partial y} \\ \dfrac{\partial u}{\partial y} + \dfrac{\partial v}{\partial x} \end{Bmatrix} + \begin{bmatrix} D_{11}^s & D_{12}^s & 0 \\ D_{11}^s & D_{12}^s & 0 \\ 0 & 0 & D_{66}^s \end{bmatrix} \begin{Bmatrix} -\dfrac{\partial^2 w_b}{\partial x^2} \\ \dfrac{\partial^2 w_b}{\partial y^2} \\ -2\dfrac{\partial^2 w_b}{\partial x \partial y} \end{Bmatrix}$$
$$+ \begin{bmatrix} H_{11}^s & H_{12}^s & 0 \\ H_{11}^s & H_{12}^s & 0 \\ 0 & 0 & H_{66}^s \end{bmatrix} \begin{Bmatrix} -\dfrac{\partial^2 w_s}{\partial x^2} \\ \dfrac{\partial^2 w_s}{\partial y^2} \\ -2\dfrac{\partial^2 w_s}{\partial x \partial y} \end{Bmatrix} \tag{32}$$

$$\begin{Bmatrix} Q_{xz} \\ Q_{yz} \end{Bmatrix} = \begin{bmatrix} A_{44}^s & 0 \\ 0 & A_{55}^s \end{bmatrix} \begin{Bmatrix} \dfrac{\partial w_s}{\partial x} \\ \dfrac{\partial w_s}{\partial y} \end{Bmatrix} \tag{33}$$

herein the cross-sectional rigidities are defined as follows:

$$(A_{ij}, B_{ij}, B_{ij}^s, D_{ij}, D_{ij}^s, H_{ij}^s) = \sum_{k=1}^{N_L} \int_{z(k)}^{z(k+z)} C_{ij}^{(k)} (1, z, f, z^2, zf, f^2) dz, \; (i,j) = 1,2,6 \tag{34}$$

and

$$A_{44}^s = A_{55}^s = \sum_{k=1}^{N_L} \int_{z(k)}^{z(k+z)} C_{55}^{(k)} g^2 dz \tag{35}$$

According to ENDM, and inserting Eqs. (30)-(33) into Eqs. (26)-(29), the following equations of wave motion in which size-dependent behavior are considered can be obtained in terms of displacements according to the following forms:

$$\begin{aligned} &A_{11}d_{11}u_0 + A_{66}d_{22}u_0 + (A_{12}+A_{66})d_{12}v_0 - B_{11}d_{111}w_b \\ &-(B_{12}+2B_{66})d_{122}w_b - B_{11}^s d_{111}w_s - (B_{12}^s + 2B_{66}^s)d_{122}w_s \\ &= \mathcal{L}_\mu (I_0 \frac{\partial^2 u_0}{\partial t^2} - I_1 d_1 \frac{\partial^2 w_b}{\partial t^2} - J_1 d_1 \frac{\partial^2 w_s}{\partial t^2}) = 0 \end{aligned} \tag{36}$$

$$\begin{aligned} &A_{22}d_{22}v_0 + A_{66}d_{11}v_0 + (A_{12}+A_{66})d_{12}u_0 - B_{22}d_{222}w_b \\ &-(B_{12}+2B_{66})d_{112}w_b - B_{22}^s d_{222}w_s - (B_{12}^s + 2B_{66}^s)d_{112}w_s \\ &= \mathcal{L}_\mu (I_0 \frac{\partial^2 v_0}{\partial t^2} - I_1 d_2 \frac{\partial^2 w_b}{\partial t^2} - J_1 d_2 \frac{\partial^2 w_s}{\partial t^2}) = 0 \end{aligned} \tag{37}$$

$$\begin{aligned} &B_{11}d_{111}u_0 + (B_{12}+2B_{66})d_{122}u_0 + (B_{12}+2B_{66})d_{122}v_0 + B_{22}d_{222}v_0 \\ &-D_{11}d_{1111}w_b - 2(D_{12}+2D_{66})d_{1122}w_b - D_{22}d_{2222}w_b - D_{11}^s d_{1111}w_s \\ &-2(D_{12}^s + 2D_{66}^s)d_{1122}w_s - D_{22}^s d_{2222}w_s + \mathcal{L}_\mu(-(\frac{k_l k_u}{k_l + k_u})(w_b + w_s) \\ &+(\frac{k_s k_u}{k_l + k_u} + \eta h H_x^2)(d_{11}w + d_{22}(w_b + w_s))) \\ &= \mathcal{L}_\mu (I_0 (\frac{\partial^2 w_b}{\partial t^2} + \frac{\partial^2 w_s}{\partial t^2}) + I_1 (d_1 \frac{\partial^2 u_0}{\partial t^2} + d_2 \frac{\partial^2 v_0}{\partial t^2}) \\ &-I_2 (d_{11} \frac{\partial^2 w_b}{\partial t^2} + d_{22} \frac{\partial^2 w_b}{\partial t^2}) - J_2 (d_{11} \frac{\partial^2 w_s}{\partial t^2} + d_{22} \frac{\partial^2 w_s}{\partial t^2})) = 0 \end{aligned} \tag{38}$$

$$\begin{aligned} &B_{11}^s d_{111}u_0 + (B_{12}^s + 2B_{66}^s)d_{122}u_0 + (B_{12}^s + 2B_{66}^s)d_{122}v_0 + B_{22}^s d_{222}v_0 \\ &-D_1^s d_{1111}w_b - 2(D_{12}^s + 2D_{66}^s)d_{1122}w_b - D_{22}^s d_{2222}w_b - H_{11}^s d_{1111}w_s \\ &-2(H_{12}^s + 2H_{66}^s)d_{1122}w_s - H_{22}^s d_{2222}w_s + A_{44}^s d_{11}w_s + A_{55}^s d_{22}w_s \\ &+\mathcal{L}_\mu(-(\frac{k_l k_u}{k_l + k_u})(w_b + w_s) + (\frac{k_s k_u}{k_l + k_u} + \eta h H_x^2)(d_{11}w + d_{22}(w_b + w_s))) \\ &= \mathcal{L}_\mu (I_0 (\frac{\partial^2 w_b}{\partial t^2} + \frac{\partial^2 w_s}{\partial t^2}) + J_1 (d_1 \frac{\partial^2 u_0}{\partial t^2} + d_2 \frac{\partial^2 v_0}{\partial t^2}) - J_2 (d_{11} \frac{\partial^2 w_b}{\partial t^2} + d_{22} \frac{\partial^2 w_b}{\partial t^2}) \\ &-K_2 (d_{11} \frac{\partial^2 w_s}{\partial t^2} + d_{22} \frac{\partial^2 w_s}{\partial t^2})) = 0 \end{aligned} \tag{39}$$

in which d_i, d_{ij}, d_{ijl}, and d_{ijlm} are the following differential operators:

$$\begin{aligned} &d_i = \frac{\partial}{\partial x_i}, \; d_{ij} = \frac{\partial^2}{\partial x_i \partial x_j}, \; d_{ijl} = \frac{\partial^3}{\partial x_i \partial x_j \partial x_l} \\ &d_{ijlm} = \frac{\partial^4}{\partial x_i \partial x_j \partial x_l \partial x_m}, \quad (i,j,l,m = 1,2) \end{aligned} \tag{40}$$

and $\mathcal{L}_\mu = (1 - \mu^2 (d_{11} + d_{22}))$.

4. Solution procedure

Here an analytical technique using harmonic series is performed to solve the wave propagation problem. Following relations are considered based on Taylor series as follows

$$\begin{aligned} u_0 &= A_1 \exp i\left(xk_x + yk_y - \omega t\right) \\ v_0 &= A_2 \exp i\left(xk_x + yk_y - \omega t\right) \\ w_b &= A_3 \exp i\left(xk_x + yk_y - \omega t\right) \\ w_s &= A_4 \exp i\left(xk_x + yk_y - \omega t\right) \end{aligned} \tag{41}$$

where A_1-A_4 represent the wave amplitude; k_x and k_y denote

the wave numbers; ω is wave frequency. By inserting Eq. (41) into Eqs. (36)-(39) gives

$$\left([K]-\omega^2[M]\right)\{\Delta\}=0 \tag{42}$$

where $[K]$ and $[M]$ are respectively the stiffness matrix and the mass matrix.

The wave frequency can be calculated by setting the following determinant to zero,

$$\left|[K]-\omega^2[M]\right|=0 \tag{43}$$

Note that: the phase velocity can be defined as

$$C=\omega/k \tag{44}$$

herein it is assumed that $k=k_x=k_y$.

5. Numerical results and discussions

In the current work, based on a higher-order shear deformation refined plate theory and ENDM, size-dependent wave characteristics of the GNPs reinforced nanoplates resting on Kerr foundation is investigated considering in-plane magnetic field effects.

Initially, the accuracy of the present solution is shown by comparing the obtained phase velocity with those reported by (Karami, Shahsavari *et al*. 2018) where the second-order plate theory was used and the results are illustrated in Fig. 3. At first sight, a good agreement can be seen for two different distance modes of wave propagation. It is interesting to note that (Fourn, Atmane *et al*. 2018) previously showed that the refined plate model prepare an excellent achievement for analysis of wave propagation.

Herein we use an epoxy-matrix with following material properties: Young modulus E_M=3GPa, Poisson's ratio ν_M=0.34, and density ρ_M=1200kg/m^3. Further, material properties of reinforcements are considered as a GNPs with E_{GNP}=1.01TPa, ν_{GNP}=0.186, ρ=1060kg/m^3. The thickness of the nanoplate is h=20 nm, and is created of GNPs against length l_{GNP}=3 nm, thickness h_{GNP}=0.7 nm, width w_{GNP}=1.8 nm (Liu, Ming *et al*. 2007).

Moreover, to show the accuracy of the present model to study the GNPs reinforced composite plates, non-dimensional natural frequencies of the plate is compared with those reported by (Song, Kitipornchai *et al*. 2017) and (Arefi, Bidgoli *et al*. 2018), and then the results are tabulated in Table 1. It is easily observed that there is a closeness between the two different mathematical models.

To investigate the size-dependent behavior of nanostructure systems, Fig. 4 is plotted. Fig. 4 demonstrates the nonlocality effect on the GNPs reinforced composite nanoplates with UD and FG distributions patterns. It is concluded that the nonlocality has the same effects on the wave characteristics such that by increasing the nonlocal parameter, phase velocity will decrease. What is more important would be that this trend is highlighted for the bigger value of wave number. All of mentioned results are the same for both methods of reinforcements.

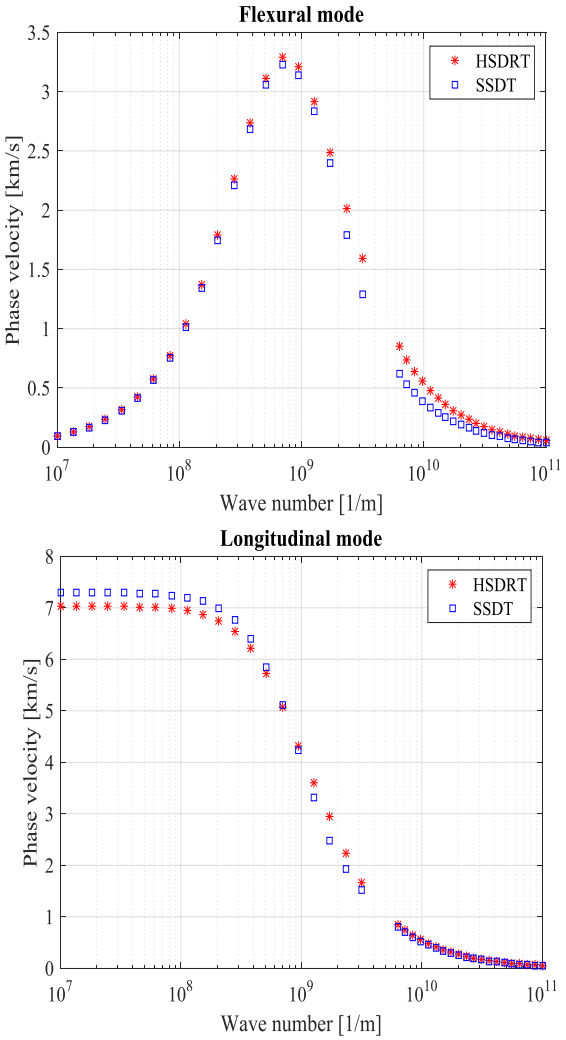

Fig. 3 The dispersion curves for isotropic rectangular nanoplates.

Table 1 Comparative assessment of the non-dimensional natural frequencies based on different patterns

Model	Pure Epoxy	UD	FG
*a	0.0584	0.1216	0.1118
*b	0.0584	0.1216	0.1118
Present	0.05843	0.12158	0.11178

*a: Ref. (Song, Kitipornchai *et al*. 2017); *b: Ref. (Arefi, Bidgoli *et al*. 2018)

Weight fraction effect (g^*_{GNP}) on the phase velocity of two different distance modes of wave propagation with respect to wave number is demonstrated in Fig. 5. The results are obtained for UD as well as FG-A patterns of reinforcements. It is easily observable that increasing weight fraction leads to an increment on the value of phase velocity for both of distance modes of propagation. Hence, the lowest phase velocity in the both modes of propagation is for the pure epoxy. This parameter plays more important role on the results of longitudinal waves. Also, it is observed that the impact of weight fraction on the results depends considerably on the wave number.

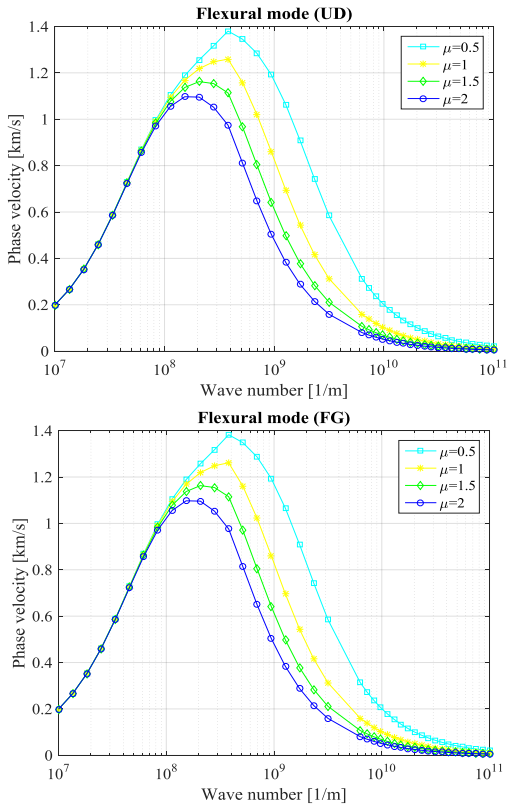

Fig. 4 The effects of nonlocal parameter on the dispersion curve of GNPs reinforced composite nanoplates (h=20 nm, g^*_{GNP}=1%, N_l=10)

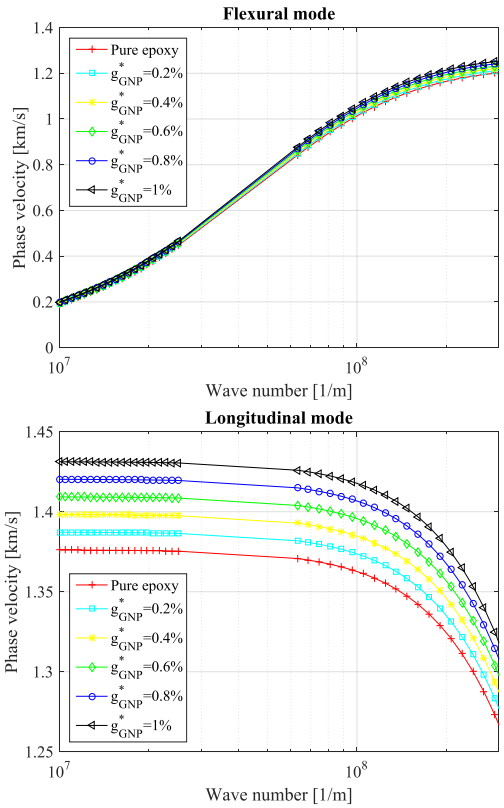

Fig. 5 The effects of weight fraction (g^*_{GNP}) on the dispersion curve of GNPs reinforced composite nanoplates, with a fixed FG pattern (h=20 nm, μ=1 nm, N_l=10)

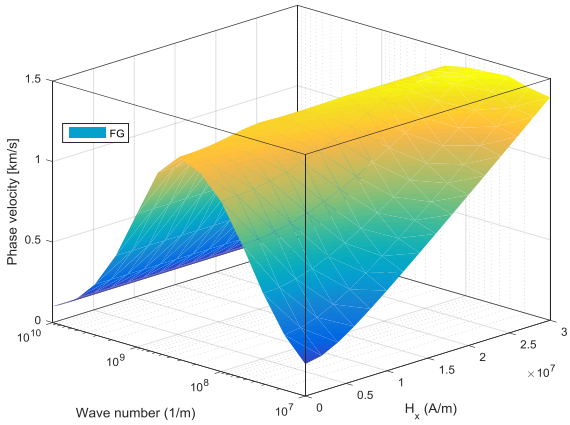

Fig. 6 The effects of magnetic potential on the dispersion curve of GNPs reinforced composite nanoplates, with a fixed FG pattern (h=20 nm, μ=1 nm, N_l=10).

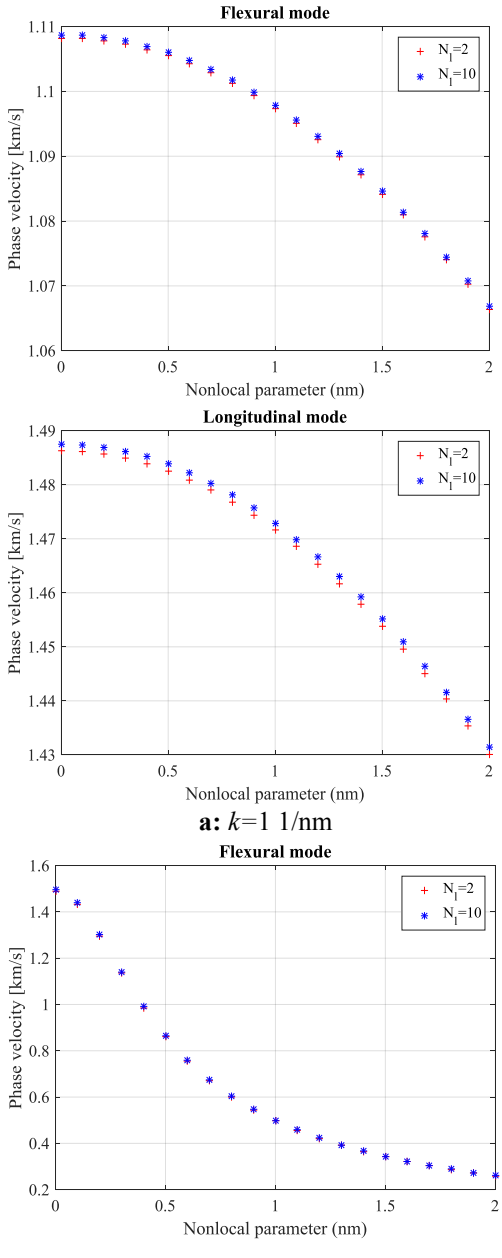

a: k=1 1/nm

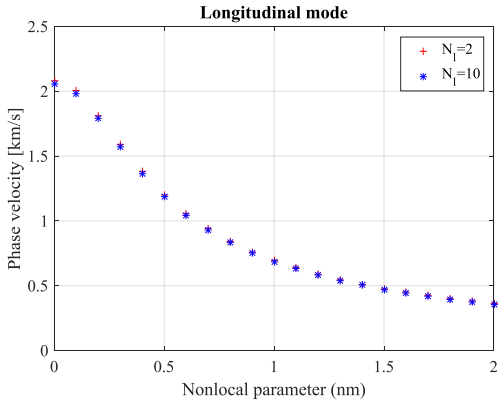

b: k=2 1/nm

Fig. 7 The effects of number of layers (N_L) on the dispersion curve of GNPs reinforced composite nanoplates, with a fixed FG pattern according to different fixed wave numbers (h=20 nm, g^*_{GNP}=2%).

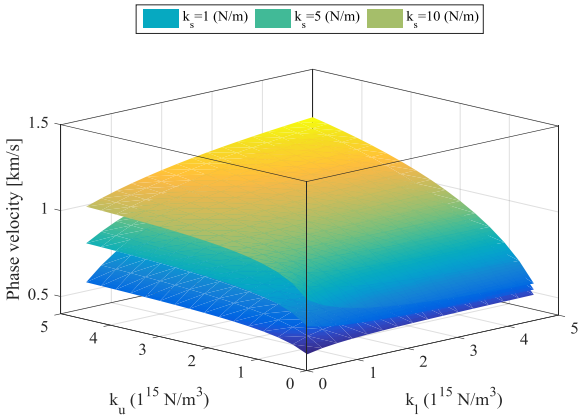

Fig. 8 The effects of Kerr foundation on the flexural dispersion curves of GNPs reinforced composite nanoplates with a fixed FG pattern (h=20 nm, g^*_{GNP}=1%, μ=1 nm).

In-plane magnetic field effect (as an external physical force) on the wave propagation of composite nanoplates with a fixed FG pattern is demonstrated in Fig. 6. The results are obtained with respect to the wave number as well as magnetic field intensity and show by a 3D graphical form. By closer examination could be seen that the magnetic field has more effect on the results when the wave number is very small (k<0.1 1/nm).

One of the important parameters in the investigation of reinforced structures with GPNs is the number of layers (N_L). Fig. 7 shows the effect of the layer number. In this way, the impact of the layer number with respect to nonlocal parameters as well as two fixed wave number is investigated. It is interesting to note that the number of layers is in relation with wave number because for both two different distance modes by changing wave number the effect of the layer number is changed. If we want to express it differently, it means that in the wave number 1 1/nm, with increasing number of layers in both of the different modes, phase velocity will be increased, but in the wave number 2 1/nm, increasing the number of layers, leads a decrement in the phase velocity for the longitudinal mode, while in the flexural mode the phase velocity is reduced (it can be said to be almost unchanged).

As the last step of the present investigation, the impact of Kerr foundation on the phase velocity variations of the GNPs reinforced nanoplates is illustrated in Fig. 8 when k=0.1 1/nm. The FG reinforcements distribution pattern is utilized. It can be seen that the effect of upper linear layer stiffness on the phase velocity of the nanoplate is more than lower linear layer once. Further, it is concluded that the shear layer of foundation plays prominent role on the results of the structure in comparison with linear layers.

6. Conclusions

This article studies wave propagation behavior of a GNPs reinforced composite nanoplates resting on Kerr foundation under in-plane magnetic field by developing a higher-order refined plate model and ENDM. Using observation, it can be concluded that nonlocal effects cause to smaller phase velocities for each pattern and the impact of nonlocality depends on the wave number. The phase velocities may decrease with the reduction in weight fraction percentage. Moreover, an increase in the number of the layers leads to a reduction in the nanoplate rigidity and magnitude of phase velocity for a specific wave number (k=1 1/nm). Furthermore, the longitudinal wave mode always has bigger phase velocity than flexural wave mode. Another interesting point would be that increasing the magnetic field intensity leads an increase in the results of composite nanoplates reinforced with GNPs. Moreover, the influences of the Kerr foundation mostly affected by the shear layer of the foundation.

References

Affdl, J.H. and Kardos, J. (1976), "The Halpin-Tsai equations: a review", *Polym. Eng. Sci.*, **16**(5), 344-352. https://doi.org/10.1002/pen.760160512.

Akgöz, B. and Civalek, Ö. (2014), "Longitudinal vibration analysis for microbars based on strain gradient elasticity theory", *J. Vib. Control.*, **20**(4), 606-616. https://doi.org/10.1177/1077546312463752.

Alimirzaei, S., Mohammadimehr, M. and Tounsi, A. (2019), "Nonlinear analysis of viscoelastic micro-composite beam with geometrical imperfection using FEM: MSGT electro-magneto-elastic bending, buckling and vibration solutions", *Struct. Eng. Mech.*, **71**(5), 485-502. https://doi.org/10.12989/sem.2019.71.5.485.

Arefi, M., Bidgoli, E.M.-R., Dimitri, R. and Tornabene, F. (2018), "Free vibrations of functionally graded polymer composite nanoplates reinforced with graphene nanoplatelets", *Aerosp. Sci. Technol.*, **81** 108-117. https://doi.org/10.1016/j.ast.2018.07.036.

Bakhadda, B., Bouiadjra, M.B., Bourada, F., Bousahla, A.A., Tounsi, A. and Mahmoud, S. (2018), "Dynamic and bending analysis of carbon nanotube-reinforced composite plates with elastic foundation", *Wind Struct.*, **27**(5), 311-324. https://doi.org/10.12989/was.2018.27.5.311.

Barati, M.R. and Shahverdi, H. (2017), "Hygro-thermal vibration analysis of graded double-refined-nanoplate systems using

hybrid nonlocal stress-strain gradient theory", *Compos. Struct*., **176** 982-995. https://doi.org/10.1016/j.compstruct.2017.06.004.

Bellifa, H., Benrahou, K.H., Bousahla, A.A., Tounsi, A. and Mahmoud, S. (2017), "A nonlocal zeroth-order shear deformation theory for nonlinear postbuckling of nanobeams", *Struct. Eng. Mech.,*. **62**(6), 695-702. https://doi.org/10.12989/sem.2017.62.6.695.

Bensaid, I. and Bekhadda, A. (2018), "Thermal stability analysis of temperature dependent inhomogeneous size-dependent nano-scale beams", *Adv. Mater. Res. J.,* **7**(1), 363-378. https://doi.org/10.12989/amr.2018.7.1.001.

Bensaid, I., Bekhadda, A. and Kerboua, B. (2018), "Dynamic analysis of higher order shear-deformable nanobeams resting on elastic foundation based on nonlocal strain gradient theory", *Adv. Nano Res.,* **6**(3), 279-298. https://doi.org/10.12989/anr.2018.6.3.279.

Berghouti, H., Adda Bedia, E., Benkhedda, A. and Tounsi, A. (2019), "Vibration analysis of nonlocal porous nanobeams made of functionally graded material", *Adv. Nano Res.,* **7**(5), 351-364. https://doi.org/10.12989/anr.2019.7.5.351.

Bouadi, A., Bousahla, A.A., Houari, M.S.A., Heireche, H. and Tounsi, A. (2018), "A new nonlocal HSDT for analysis of stability of single layer graphene sheet", *Adv. Nano Res.,* **6**(2), 147-162. https://doi.org/10.12989/anr.2018.6.2.147.

Boukhlif, Z., Bouremana, M., Bourada, F., Bousahla, A.A., Bourada, M., Tounsi, A. and Al-Osta, M.A. (2019), "A simple quasi-3D HSDT for the dynamics analysis of FG thick plate on elastic foundation", *Steel Compos. Struct.,* **31**(5), 503-516. https://doi.org/10.12989/scs.2019.31.5.503.

Boulefrakh, L., Hebali, H., Chikh, A., Bousahla, A.A., Tounsi, A. and Mahmoud, S. (2019), "The effect of parameters of visco-Pasternak foundation on the bending and vibration properties of a thick FG plate", *Geomech. Eng.,* **18**(2), 161-178. https://doi.org/10.12989/gae.2019.18.2.161.

Bounouara, F., Benrahou, K.H., Belkorissat, I. and Tounsi, A. (2016), "A nonlocal zeroth-order shear deformation theory for free vibration of functionally graded nanoscale plates resting on elastic foundation", *Steel Compos. Struct.,* **20**(2), 227-249. https://doi.org/10.12989/scs.2016.20.2.227.

Bourada, F., Amara, K., Bousahla, A.A., Tounsi, A. and Mahmoud, S. (2018), "A novel refined plate theory for stability analysis of hybrid and symmetric S-FGM plates", *Struct. Eng. Mech.,* **68**(6), 661-675. https://doi.org/10.12989/sem.2018.68.6.661.

Bourada, F., Bousahla, A.A., Bourada, M., Azzaz, A., Zinata, A. and Tounsi, A. (2019), "Dynamic investigation of porous functionally graded beam using a sinusoidal shear deformation theory", *Wind Struct*., **28**(1), 19-30. https://doi.org/10.12989/was.2019.28.1.019.

Boutaleb, S., Benrahou, K.H., Bakora, A., Algarni, A., Bousahla, A.A., Tounsi, A., Tounsi, A. and Mahmoud, S. (2019), "Dynamic analysis of nanosize FG rectangular plates based on simple nonlocal quasi 3D HSDT", *Adv. Nano Res.,* **7**(3), 191. https://doi.org/10.12989/anr.2019.7.3.191.

Chaabane, L.A., Bourada, F., Sekkal, M., Zerouati, S., Zaoui, F.Z., Tounsi, A., Derras, A., Bousahla, A.A. and Tounsi, A. (2019), "Analytical study of bending and free vibration responses of functionally graded beams resting on elastic foundation", *Struct. Eng. Mech..,* **71**(2), 185-196. https://doi.org/10.12989/sem.2019.71.2.185.

Dash, S., Mehar, K., Sharma, N., Mahapatra, T.R. and Panda, S.K. (2018), "Modal analysis of FG sandwich doubly curved shell structure", *Struct. Eng. Mech..,* **68**(6), 721-733. https://doi.org/10.12989/sem.2018.68.6.721.

Dash, S., Mehar, K., Sharma, N., Mahapatra, T.R. and Panda, S.K. (2019), "Finite element solution of stress and flexural strength of functionally graded doubly curved sandwich shell panel", *Earthq. Struct.,* **16**(1), 55-67. https://doi.org/10.12989/eas.2019.16.1.055.

Draoui, A., Zidour, M., Tounsi, A. and Adim, B. (2019). "Static and dynamic behavior of nanotubes-reinforced sandwich plates using (FSDT)", *J. Nano Res.,* https://doi.org/10.4028/www.scientific.net/JNanoR.57.117.

Dutta, G., Panda, S.K., Mahapatra, T.R. and Singh, V.K. (2017), "Electro-magneto-elastic response of laminated composite plate: A finite element approach", *J. Appl. Comput. Math.,* **3**(3), 2573-2592. https://doi.org/10.1007/s40819-016-0256-6.

Ebrahimi, F., Barati, M.R. and Dabbagh, A. (2016), "A nonlocal strain gradient theory for wave propagation analysis in temperature-dependent inhomogeneous nanoplates", *J. Eng. Sci.,* **107** 169-182. https://doi.org/10.1016/j.ijengsci.2016.07.008.

Ebrahimi, F., Barati, M.R. and Zenkour, A.M. (2018), "A new nonlocal elasticity theory with graded nonlocality for thermo-mechanical vibration of FG nanobeams via a nonlocal third-order shear deformation theory", *Mech. Adv. Mater. Struct.,* **25**(6), 512-522. https://doi.org/10.1080/15376494.2017.1285458.

Eringen, A.C. (1983), "On differential equations of nonlocal elasticity and solutions of screw dislocation and surface waves", *J. Appl. Phys.,* **54**(9), 4703-4710. https://doi.org/10.1063/1.332803.

Eringen, A.C. and Edelen, D. (1972), "On nonlocal elasticity", *J. Eng. Sci.,* **10**(3), 233-248. https://doi.org/10.1016/0020-7225(72)90039-0.

Farokhi, H. and Ghayesh, M.H. (2015), "Nonlinear dynamical behaviour of geometrically imperfect microplates based on modified couple stress theory", *J. Mech. Sci.,* **90** 133-144. https://doi.org/10.1016/j.ijmecsci.2014.11.002.

Fourn, H., Atmane, H.A., Bourada, M., Bousahla, A.A., Tounsi, A. and Mahmoud, S. (2018), "A novel four variable refined plate theory for wave propagation in functionally graded material plates", *Steel Compos. Struct.,* **27**(1), 109-122. https://doi.org/10.12989/scs.2018.27.1.109.

Gao, Y., Xiao, W.-S. and Zhu, H. (2019), "Nonlinear vibration of functionally graded nano-tubes using nonlocal strain gradient theory and a two-steps perturbation method", *Struct. Eng. Mech.,*. **69**(2), 205-219. https://doi.org/10.12989/sem.2019.69.2.205.

Ghayesh, M.H., Amabili, M. and Farokhi, H. (2013), "Nonlinear forced vibrations of a microbeam based on the strain gradient elasticity theory", *J. Eng. Sci.,* **63** 52-60. https://doi.org/10.1016/j.ijengsci.2012.12.001.

Ghayesh, M.H., Amabili, M. and Farokhi, H. (2013), "Three-dimensional nonlinear size-dependent behaviour of Timoshenko microbeams", *J. Eng. Sci.,* **71** 1-14. https://doi.org/10.1016/j.ijengsci.2013.04.003.

Ghayesh, M.H. and Farokhi, H. (2018), "Size-dependent internal resonances and modal interactions in nonlinear dynamics of microcantilevers", *J. Mech. Mater. Design.,* **14**(1), 127-140. https://doi.org/10.1007/s10999-017-9365-6.

Ghayesh, M.H., Farokhi, H. and Alici, G. (2016), "Size-dependent performance of microgyroscopes", *J. Eng. Sci.,* **100** 99-111. https://doi.org/10.1016/j.ijengsci.2015.11.003.

Ghayesh, M.H., Farokhi, H., Gholipour, A., Hussain, S. and Arjomandi, M. (2017), "Resonance responses of geometrically imperfect functionally graded extensible microbeams", *J. Comput. Nonlinear Dynam.,* **12**(5), 051002. https://doi.org/10.1115/1.4035214.

Ghayesh, M.H., Farokhi, H., Gholipour, A. and Tavallaeinejad, M. (2018), "Nonlinear oscillations of functionally graded microplates", *J. Eng. Sci.,* **122** 56-72. https://doi.org/10.1016/j.ijengsci.2017.03.014.

Gholami, R. and Ansari, R. (2018), "On the Nonlinear Vibrations of Polymer Nanocomposite Rectangular Plates Reinforced by Graphene Nanoplatelets: A Unified Higher-Order Shear Deformable Model", *Iranian J. Sci. Technol. Transactions. Mech. Eng.*. 1-18. https://doi.org/10.1007/s40997-018-0182-9.

Hosseini, M., Bahaadini, R. and Jamali, B. (2018), "Nonlocal instability of cantilever piezoelectric carbon nanotubes by considering surface effects subjected to axial flow", *J. Vib. Control*. **24**(9), 1809-1825. https://doi.org/10.1177/1077546316669063.

Jawaid, M., Thariq, M. and Saba, N. (2018), *Modelling of Damage Processes in Biocomposites, Fibre-Reinforced Composites and Hybrid Composites*, Woodhead Publishing. https://doi.org/10.1016/C2016-0-04450-9.

Kaghazian, A., Hajnayeb, A. and Foruzande, H. (2017), "Free vibration analysis of a piezoelectric nanobeam using nonlocal elasticity theory", *Struct. Eng. Mech.,*. **61**(5), 617-624. https://doi.org/10.12989/sem.2017.61.5.617.

Kar, V., Panda, S., Tripathy, P., Jayakrishnan, K., Rajesh, M., Karakoti, A. and Manikandan, M. (2019), *Deformation Characteristics of Functionally Graded Composite Panels Using Finite Element Approximation*, Elsevier, Germany. https://doi.org/10.1016/B978-0-08-102289-4.00012-6.

Karami, B., Janghorban, M. and Li, L. (2018), "On guided wave propagation in fully clamped porous functionally graded nanoplates", *Acta Astronautica*. **143** 380-390. https://doi.org/10.1016/j.actaastro.2017.12.011.

Karami, B., Janghorban, M., Shahsavari, D. and Tounsi, A. (2018), "A size-dependent quasi-3D model for wave dispersion analysis of FG nanoplates", *Steel Compos. Struct.,* **28**(1), 99-110. https://doi.org/10.12989/sem.2019.69.5.487.

Karami, B., Janghorban, M. and Tounsi, A. (2017), "Effects of triaxial magnetic field on the anisotropic nanoplates", *Steel Compos. Struct.,* **25**(3), 361-374. https://doi.org/10.12989/scs.2017.25.3.361.

Karami, B., Janghorban, M. and Tounsi, A. (2018), "Nonlocal strain gradient 3D elasticity theory for anisotropic spherical nanoparticles", *Steel Compos. Struct.,* **27**(2), 201-216. https://doi.org/10.12989/scs.2018.27.2.201.

Karami, B., Janghorban, M. and Tounsi, A. (2018), "Variational approach for wave dispersion in anisotropic doubly-curved nanoshells based on a new nonlocal strain gradient higher order shell theory", *Thin Wall. Struct.,* **129** 251-264. https://doi.org/10.1016/j.tws.2018.02.025.

Karami, B., Janghorban, M. and Tounsi, A. (2019), "Wave propagation of functionally graded anisotropic nanoplates resting on Winkler-Pasternak foundation", *Struct. Eng. Mech.,* **70**(1), 55-66. https://doi.org/10.12989/sem.2019.70.1.055.

Karami, B., Shahsavari, D. and Janghorban, M. (2018), "Wave propagation analysis in functionally graded (FG) nanoplates under in-plane magnetic field based on nonlocal strain gradient theory and four variable refined plate theory", *Mech. Adv. Mater. Struct.,* **25**(12), 1047-1057. https://doi.org/10.1080/15376494.2017.1323143.

Karami, B., Shahsavari, D., Janghorban, M. and Li, L. (2018), "Wave dispersion of mounted graphene with initial stress", *Thin Wall. Struct.,* **122** 102-111. https://doi.org/10.1016/j.tws.2017.10.004.

Karami, B., Shahsavari, D., Janghorban, M. and Tounsi, A. (2019), "Resonance behavior of functionally graded polymer composite nanoplates reinforced with graphene nanoplatelets", *J. Mech. Sci.,* **156** 94-105. https://doi.org/10.1016/j.ijmecsci.2019.03.036.

Khetir, H., Bouiadjra, M.B., Houari, M.S.A., Tounsi, A. and Mahmoud, S. (2017), "A new nonlocal trigonometric shear deformation theory for thermal buckling analysis of embedded nanosize FG plates", *Struct. Eng. Mech.,* **64**(4), 391-402. https://doi.org/10.12989/sem.2017.64.4.391.

Kocaturk, T. and Akbas, S.D. (2013), "Wave propagation in a microbeam based on the modified couple stress theory", *Struct. Eng. Mech.,* **46**(3), 417-431. https://doi.org/10.12989/sem.2013.46.3.417.

Li, L. and Hu, Y. (2017), "Torsional vibration of bi-directional functionally graded nanotubes based on nonlocal elasticity theory", *Compos. Struct.,* **172** 242-250. https://doi.org/10.1016/j.compstruct.2017.03.097.

Liu, F., Ming, P. and Li, J. (2007), "Ab initio calculation of ideal strength and phonon instability of graphene under tension", *Physical Review B*. **76**(6), 064120. https://doi.org/10.1103/PhysRevB.76.064120.

Mahmoudi, A., Benyoucef, S., Tounsi, A., Benachour, A., Adda Bedia, E.A. and Mahmoud, S. (2019), "A refined quasi-3D shear deformation theory for thermo-mechanical behavior of functionally graded sandwich plates on elastic foundations", *J. Sandwich Struct. Mater.,* **21**(6), 1906-1929. https://doi.org/10.1177/1099636217727577.

Medani, M., Benahmed, A., Zidour, M., Heireche, H., Tounsi, A., Bousahla, A.A., Tounsi, A. and Mahmoud, S. (2019), "Static and dynamic behavior of (FG-CNT) reinforced porous sandwich plate using energy principle", *Steel Compos. Struct.,* **32**(5), 595-610. https://doi.org/10.12989/scs.2019.32.5.595.

Mehar, K., Mahapatra, T.R., Panda, S.K., Katariya, P.V. and Tompe, U.K. (2018), "Finite-element solution to nonlocal elasticity and scale effect on frequency behavior of shear deformable nanoplate structure", *J. Eng. Mech.,* **144**(9), https://doi.org/10.1061/(ASCE)EM.1943-7889.0001519.

Mehar, K. and Panda, S.K. (2016), "Geometrical nonlinear free vibration analysis of FG-CNT reinforced composite flat panel under uniform thermal field", *Compos. Struct.,* **143** 336-346. https://doi.org/10.1016/j.compstruct.2016.02.038.

Mehar, K. and Panda, S.K. (2019), "Multiscale modeling approach for thermal buckling analysis of nanocomposite curved structure", *Adv. Nano Res.,* **7**(3), 181. https://doi.org/10.12989/anr.2019.7.3.181.

Mehar, K. and Panda, S.K. (2019), "Theoretical deflection analysis of multi-walled carbon nanotube reinforced sandwich panel and experimental verification", *Compos. Part B Eng.,* **167** 317-328. https://doi.org/10.1016/j.compositesb.2018.12.058.

Mehar, K., Panda, S.K., Devarajan, Y. and Choubey, G. (2019), "Numerical buckling analysis of graded CNT-reinforced composite sandwich shell structure under thermal loading", *Compos. Struct.,* **216** 406-414. https://doi.org/10.1016/j.compstruct.2019.03.002.

Meksi, R., Benyoucef, S., Mahmoudi, A., Tounsi, A., Adda Bedia, E.A. and Mahmoud, S. (2019), "An analytical solution for bending, buckling and vibration responses of FGM sandwich plates", *J. Sandwich Struct. Mater.,* **21**(2), 727-757. https://doi.org/10.1177/1099636217698443.

Mercan, K. and Civalek, Ö. (2017), "Buckling analysis of Silicon carbide nanotubes (SiCNTs) with surface effect and nonlocal elasticity using the method of HDQ", *Compos. Part B Eng.,* **114** 34-45. https://doi.org/10.1016/j.compositesb.2017.01.067.

Mokhtar, Y., Heireche, H., Bousahla, A.A., Houari, M.S.A., Tounsi, A. and Mahmoud, S. (2018), "A novel shear deformation theory for buckling analysis of single layer graphene sheet based on nonlocal elasticity theory", *Smart Struct. Syst.,* **21**(4), 397-405. https://doi.org/10.12989/sss.2018.21.4.397.

Papargyri-Beskou, S., Polyzos, D. and Beskos, D. (2009), "Wave dispersion in gradient elastic solids and structures: a unified treatment", *J. Solids Struct.,***46**(21), 3751-3759. https://doi.org/10.1016/j.ijsolstr.2009.05.002.

Rad, A.B. (2015), "Thermo-elastic analysis of functionally graded circular plates resting on a gradient hybrid foundation", *Appl. Math. Comput.,* **256** 276-298. https://doi.org/10.1016/j.amc.2015.01.026.

Rafiee, M.A., Rafiee, J., Wang, Z., Song, H., Yu, Z.-Z. and Koratkar, N. (2009), "Enhanced mechanical properties of nanocomposites at low graphene content", *ACS Nano*., **3**(12), 3884-3890. https://pubs.acs.org/doi/abs/10.1021/nn9010472.

Rahmani, O., Deyhim, S., Hosseini, S. and Hossein, A. (2018), "Size dependent bending analysis of micro/nano sandwich structures based on a nonlocal high order theory", *Steel Compos. Struct.,* **27**(3), 371-388. https://doi.org/10.12989/scs.2018.27.3.371.

Ramteke, P.M., Panda, S.K. and Sharma, N. (2019), "Effect of

grading pattern and porosity on the eigen characteristics of porous functionally graded structure", *Steel Compos. Struct.,* **33**(6), 865. https://doi.org/10.12989/scs.2019.33.6.865.

Romano, G. and Barretta, R. (2017), "Nonlocal elasticity in nanobeams: the stress-driven integral model", *J. Eng. Sci.,* **115**, 14-27. https://doi.org/10.1016/j.ijengsci.2017.03.002.

Romano, G., Barretta, R., Diaco, M. and de Sciarra, F.M. (2017), "Constitutive boundary conditions and paradoxes in nonlocal elastic nanobeams", *J. Mech. Sci.,* **121**, 151-156. https://doi.org/10.1016/j.ijmecsci.2016.10.036.

Sahmani, S., Aghdam, M.M. and Rabczuk, T. (2018), "Nonlocal strain gradient plate model for nonlinear large-amplitude vibrations of functionally graded porous micro/nano-plates reinforced with GPLs", *Compos. Struct.,* **198**, 51-62. https://doi.org/10.1016/j.compstruct.2018.05.031.

Sahmani, S., Aghdam, M.M. and Rabczuk, T. (2018), "A unified nonlocal strain gradient plate model for nonlinear axial instability of functionally graded porous micro/nano-plates reinforced with graphene platelets", *Mater. Res. Express.,***5**(4), 045048. https://orcid.org/0000-0003-4129-4554.

Shahsavari, D. and Janghorban, M. (2017), "Bending and shearing responses for dynamic analysis of single-layer graphene sheets under moving load", *J. Brazilian Soc. Mech. Sci. Eng.,* **39**(10), 3849-3861. https://doi.org/10.1007/s40430-017-0863-0.

Shahsavari, D., Karami, B., Janghorban, M. and Li, L. (2017), "Dynamic characteristics of viscoelastic nanoplates under moving load embedded within visco-Pasternak substrate and hygrothermal environment", *Mater. Res. Express.,***4**(8), 085013. https://doi.org/10.1088/2053-1591/aa7d89.

Song, M., Kitipornchai, S. and Yang, J. (2017), "Free and forced vibrations of functionally graded polymer composite plates reinforced with graphene nanoplatelets", *Compos. Struct.,* **159**, 579-588. https://doi.org/10.1016/j.compstruct.2016.09.070.

Song, M., Yang, J. and Kitipornchai, S. (2018), "Bending and buckling analyses of functionally graded polymer composite plates reinforced with graphene nanoplatelets", *Compos. Part B Eng.,* **134**, 106-113. https://doi.org/10.1016/j.compositesb.2017.09.043.

Wang, L. and Zheng, S. (2018), "Nonlinear analysis of 0–3 polarized PLZT microplate based on the new modified couple stress theory", *Physica E: Low-dimensional Syst. Nanostruct.*., **96**, 94-101. https://doi.org/10.1016/j.physe.2017.10.001.

Yazid, M., Heireche, H., Tounsi, A., Bousahla, A.A. and Houari, M.S.A. (2018), "A novel nonlocal refined plate theory for stability response of orthotropic single-layer graphene sheet resting on elastic medium", *Smart Struct. Syst.,* **21**(1), 15-25. https://doi.org/10.12989/sss.2018.21.1.015.

Youcef, D.O., Kaci, A., Benzair, A., Bousahla, A.A. and Tounsi, A. (2018), "Dynamic analysis of nanoscale beams including surface stress effects", *Smart Struct. Syst.,* **21**(1), 65-74. https://doi.org/10.12989/sss.2018.21.1.065.

Zaoui, F.Z., Ouinas, D. and Tounsi, A. (2019), "New 2D and quasi-3D shear deformation theories for free vibration of functionally graded plates on elastic foundations", *Compos. Part B Eng.,* **159**, 231-247. https://doi.org/10.1016/j.compositesb.2018.09.051

Zarga, D., Tounsi, A., Bousahla, A.A., Bourada, F. and Mahmoud, S. (2019), "Thermomechanical bending study for functionally graded sandwich plates using a simple quasi-3D shear deformation theory", *Steel Compos. Struct.,* **32**(3), 389-410. https://doi.org/10.12989/scs.2019.32.3.389.

Zemri, A., Houari, M.S.A., Bousahla, A.A. and Tounsi, A. (2015), "A mechanical response of functionally graded nanoscale beam: an assessment of a refined nonlocal shear deformation theory beam theory", *Struct. Eng. Mech.,* **54**(4), 693-710. https://doi.org/10.12989/sem.2015.54.4.693.